THE JOURNAL OF PHYSICAL CHEMISTRY B

ARTICLE

pubs.acs.org/JPCB

Structural Properties of High and Low Density Water in a Supercooled Aqueous Solution of Salt

D. Corradini, M. Rovere, and P. Gallo*

Dipartimento di Fisica, Università "Roma Tre", Via della Vasca Navale 84, I-00146 Roma, Italy

ABSTRACT: We consider and compare the structural properties of bulk TIP4P water and of a sodium chloride aqueous solution in TIP4P water with concentration $c = 0.67$ mol/kg, in the metastable supercooled region. In a previous paper (Corradini, D.; Rovere, M.; Gallo, P. *J. Chem. Phys.* **2010**, *132*, 134508) we found in both systems the presence of a liquid−liquid critical point (LLCP). The LLCP is believed to be the end point of the coexistence line between a high density liquid (HDL) and a low density liquid (LDL) phase of water. In the present paper we study the different features of water−water structure in HDL and LDL both in bulk water and in the solution. We find that the ions are able to modify the bulk LDL structure, rendering water−water structure more similar to the bulk HDL case. By the study of the hydration structure in HDL and LDL, a possible mechanism for the modification of the bulk LDL structure in the solution is identified in the substitution of the oxygen by the chloride ion in oxygen coordination shells.

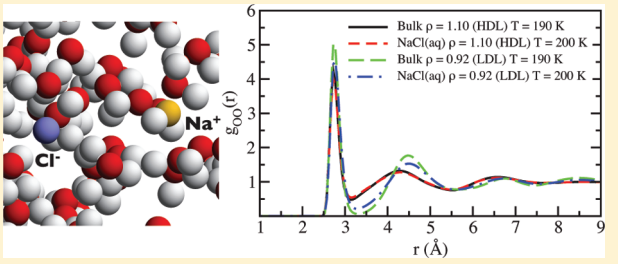

1. INTRODUCTION

The possible existence of a second critical point of water in the liquid supercooled metastable phase has been the subject of a long debate in the literature. The first hypothesis of its existence originated from the results of a computer simulation on water modeled with the ST2 potential.[1] On the basis of those results, the thermodynamic anomalies of water upon supercooling were interpreted in terms of the long-range fluctuations induced by the presence of a second critical point. This critical point would be a liquid−liquid critical point (LLCP) located at the end of the coexistence line between a low density liquid (LDL) phase and a high density liquid (HDL) phase of water. In the LLCP scenario, these liquid phases would be the counterpart, at a higher temperature, of the well-known low density amorphous (LDA) and high density amorphous (HDA) phases of glassy water. The hypothesis of a LLCP scenario for water motivated a large number of experimental, computational, and theoretical investigations.[2,3]

Different interpretations of the origin of the thermodynamic anomalies of water have been also proposed as alternatives to the LLCP scenario. In the singularity free scenario[4] the anomalies of water are due to local density fluctuations and no critical phenomena take place. Recently a critical point free scenario[5] has also been proposed in which the transition between HDL and LDL is seen as an order−disorder transition without a critical point.

A number of computer simulations, performed on supercooled water with different model potentials, confirmed the plausibility of the LLCP scenario.[6−15] There are also indications from experiments of the existence of the LLCP in bulk water.[16−19] It would be approximately located at $T \sim 220$ K at $P \sim 100$ MPa.

Because of the difficulties of performing experiments in the region where the LLCP would reside in bulk water, the possibility of observing the LLCP of water in aqueous solutions that can be more easily supercooled[20] has been recently explored theoretically[21] and in computer simulations.[22,23] Results compatible with the existence of a LLCP have also been found in aqueous solutions of salts through thermometric experiments.[24−27]

In a recent paper,[22] by means of a computer simulation study of the phase diagram, we indicated the possible detection in thermometric experiments of the LLCP in a NaCl(aq) solution. Since the detection of low and high density forms of water can also offer a viable path to the experimental detection of a LLCP, structural properties of supercooled water and aqueous solutions are of extreme interest in this context. The structure of water and of aqueous solutions can be studied with neutron diffraction using isotopic substitution[28,29] or by X-ray scattering.[30]

In the present paper we focus on the structural properties of bulk TIP4P water and of the NaCl(aq) solution with $c = 0.67$ mol/kg, in order to analyze and compare the results in HDL and LDL especially close to the LLCP. The paper is organized as follows. In section 2 the details of the computer simulations are given. In section 3 we summarize the main results obtained on the thermodynamics of bulk water and NaCl(aq), and we present the potential energy of the systems. The new results for the structural properties of the systems are presented in section 4. This section is divided in two parts: water−water structure is discussed in subsection 4A, while the hydration structure of ions is addressed in subsection 4B. Finally, conclusions are given in section 5.

Received: October 22, 2010
Revised: December 23, 2010
Published: January 26, 2011

Table 1. Ion−Ion and Ion−Water LJ Interaction Parameters[33]

atom pair	ϵ (kJ/mol)	σ (Å)
Na−Na	0.002	4.070
Na−Cl	0.079	4.045
Cl−Cl	2.971	4.020
Na−O	0.037	3.583
Cl−O	1.388	3.561

2. COMPUTER SIMULATION DETAILS

Molecular dynamics (MD) computer simulations were performed on bulk water and on NaCl(aq) with concentration c = 0.67 mol/kg. The interaction potential between pairs of particles is given by the sum of the electrostatic and the Lennard−Jones (LJ) potentials.

$$U_{ij}(r) = \frac{q_i q_j}{r} + 4\epsilon_{ij}\left[\left(\frac{\sigma_{ij}}{r}\right)^{12} - \left(\frac{\sigma_{ij}}{r}\right)^{6}\right] \quad (1)$$

Water molecules were modeled using the TIP4P potential.[31] The details about this potential are reported in the Appendix. TIP4P potential is known to well describe water properties in its liquid supercooled state[31] and also to be able to reproduce the very complex ices phase diagram.[32]

The LJ interaction parameters for the ions were taken from Jensen and Jorgensen,[33] and the ion−water interaction parameters were calculated by using geometrical mixing rules $\epsilon_{ij} = (\epsilon_{ii}\epsilon_{jj})^{1/2}$ and $\sigma_{ij} = (\sigma_{ii}\sigma_{jj})^{1/2}$. The ion−ion and ion−water parameters are reported in Table 1. These parameters were optimized for use with TIP4P water, and they well reproduce structural characteristics and free energies of hydration of the ions.[33]

Although the presence of ions would suggest the use of polarizable potentials, at the moment no joint set of polarizable potentials for water and ions have been tested to be reliable for very low temperatures.

Periodic boundary conditions were applied. The cutoff radius was set at 9 Å. Standard long-range corrections were applied for the calculation of the potential energy and the virial. The long-range electrostatic interactions were handled with the Ewald summation method. The integration time step was fixed at 1 fs.

The total number of particles contained in the simulation box is N_{tot} = 256. For bulk water $N_{wat} = N_{tot}$ = 256 while in the case of NaCl(aq) with concentration c = 0.67 mol/kg, N_{wat} = 250, and $N_{Na^+} = N_{Cl^-}$ = 3. Extensive sets of simulations were run both for bulk water and for NaCl(aq). The range of densities investigated spans from ρ = 0.83 g/cm^3 to ρ = 1.10 g/cm^3 and the range of temperatures goes from T = 350 K to T = 190 K. Temperature was controlled using a Berendsen thermostat.[34] Equilibration and production simulation times were progressively increased with the decreasing temperature. The total running times span from 0.15 ns for the highest temperatures to 30 ns for the lowest ones. The parallelized version of the DL_POLY package[35] was employed to perform the simulations. The total simulation time is ca. 6 single CPU years.

3. THERMODYNAMICS IN THE SUPERCOOLED REGION

In this section we start by summarizing the main results on the thermodynamic behavior in the supercooled region of bulk water and of NaCl(aq) obtained in ref 22, and then we analyze the behavior of the potential energy of the systems studied at different temperatures. From extensive simulations on bulk TIP4P water and on NaCl(aq) with concentration c = 0.67 mol/kg, we located the LLCP in both systems. Details about the calculation of the position of the LLCP are given in ref 22.

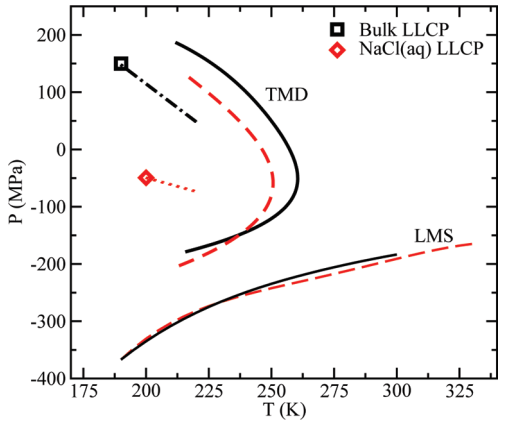

Figure 1. Comparison between the thermodynamic features of bulk water and NaCl(aq) in the supercooled region, based on the results shown in ref 22. We report the position of the LLCP and of the Widom line for bulk water (dot-dashed line) and for NaCl(aq) (dotted line). The TMD and LG-LMS lines are also shown for bulk water (solid lines) and NaCl(aq) (dashed lines).

In Figure 1 we report a comparison of the phase diagrams of the supercooled regions of bulk water and NaCl(aq) as obtained directly from MD. Together with the LLCP of the two systems, we show the Widom lines, the temperature of maximum density (TMD) lines, and the liquid−gas limit of mechanical stability (LG-LMS) lines. The Widom line can be considered an extension of the coexistence line in the one-phase region.[36,37] In bulk water the position of the LLCP is T_c = 190 K and P_c = 150 MPa. In a very recent paper[38] another estimate of the LLCP for bulk water has been performed with a TIP4P potential with modified parameters.[39] The values that the authors obtained for the critical point, T_c = 193 K and P_c = 135 MPa, and the Widom line appears substantially the same as the values that we found with the original TIP4P.[22]

Coming back to Figure 1, we can see that in NaCl(aq) the position of the LLCP moves to lower pressure and higher temperature, appearing at T_c = 200 K and P_c= −50 MPa. The TMD line of the solution lies ca. 10 K below in temperature and at slightly lower pressure with respect to bulk water. The LG-LMS instead is almost unchanged with respect to the bulk. From the comparison of the phase diagrams for these two systems, we found that the main effect of the presence of the ions is to shrink the region of existence of the LDL,[22] consistent with an observed increased solubility of ions in HDL water.[27,40]

Importantly, we also found that with a rigid shift in temperature and pressure of the phase diagram of TIP4P bulk water (not shown), that brought the TMD curve to coincide with the experimental TMD values, the LLCP in bulk water appears at T_c = 221 K and P_c = 77 MPa, close to the experimental value estimated by Mishima and Stanley,[16] $T_c \sim$ 220 K and $P_c \sim$ 100 MPa. We note that this shift in temperature is compatible with the shift between the melting line of TIP4P[41] and the melting line of real water. Recently Mishima published a new estimate of the LLCP in the bulk at $T_c \sim$ 223 K and $P_c \sim$ 50 MPa,[19] also compatible with our findings. These results confirm that TIP4P is

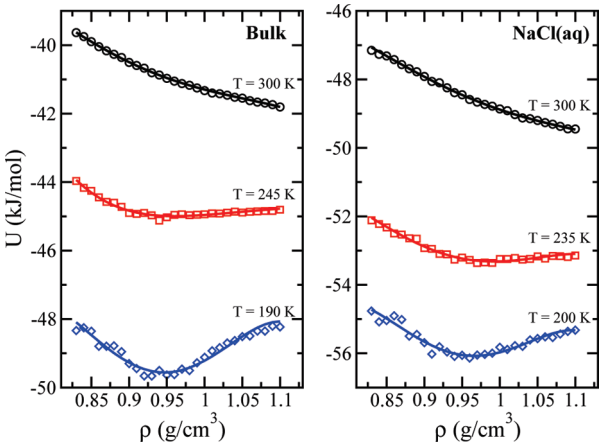

Figure 2. Potential energy per molecule as a function of the density of the system at constant temperature. For bulk water (left panel) the isotherms of the potential energy are reported at T = 300 K, T = 245 K, and T = 190 K. For NaCl(aq) (right panel), the isotherms of the potential energy are reported at T = 300 K, T = 235 K, and T = 200 K. Continuous lines are a polynomial best fits to the simulated points.

a good potential for describing the supercooled water phase diagram. The same shift applied to our ionic solution led us to predict an LLCP in NaCl(aq) located at $T_c \sim 231$ K and $P_c \sim -123$ MPa. These last values appear to be in a region accessible by experiments, being above the homogeneous nucleation temperature of the solution.[20,42]

Generally speaking, from the behavior of the potential energy U, it is also possible to extract information on the thermodynamics of a system close to a phase transition. As already pointed out in refs 8 and 15, if we examine the curvature of the configurational part of the Helmholtz free energy $A = U - TS$,

$$\left(\frac{\partial^2 A}{\partial V^2}\right)_T = \left(\frac{\partial^2 U}{\partial V^2}\right)_T - T\left(\frac{\partial^2 S}{\partial V^2}\right)_T \qquad (2)$$

it must be positive in the region of stability of an homogeneous phase. When the curvature of U is negative, the system can still be stable due to the contribution of a dominant entropic term in eq 2. At supercooled low temperatures, the stabilization induced by the entropic term can be less effective as the factor T in front of the second derivative of the entropy in eq 2 becomes progressively smaller. Thus, at low temperatures the range of volumes where $(\partial^2 U/\partial V^2)_T < 0$ corresponds to a region of reduced stability for the homogeneous liquid, where separation in two distinct phases with different densities may occur.

In Figure 2 the isotherms of the potential energy are reported for three temperatures for bulk water and NaCl(aq). We show the behavior of potential energy for ambient temperature T = 300 K, for the first temperature showing a negative curvature of U, T = 245 K in the bulk and T = 235 K in the solution, and for the LLCP temperature, T = 190 K in the bulk and T = 200 K in the solution. In both systems, at high temperature the potential energy is a positively curved function of the density and it decreases monotonically (becomes more negative) as density increases. When the temperature is decreased, a minimum is formed after which the curvature of the potential energy becomes negative. The minimum corresponds to the presence of a tetrahedrally ordered liquid with an energetically favorable configuration.[15] For the temperature corresponding to that of the LLCP, we see that in both systems the minimum becomes very deep and a maximum is suggested at high densities, indicating the possible occurrence of a second minimum at higher densities. This second minimum has been previously observed for confined bulk water[43] and for higher concentration NaCl(aq) solutions[44] and connected to the existence of two distinct liquid phases in the system, as at very low temperatures the entropic contribution is depressed and the behavior of the free energy A can be approximated with that of the potential energy U. Comparing the behavior of the potential energy of bulk water and NaCl(aq), we notice that apart from the shift in the absolute value due the presence of ions, their behavior is quite similar. Nonetheless, the minimum at low density becomes more shallow in the solution, indicating that this phase is made less stable by the presence of ions, consistent with the fact that ions stabilize the high density phase.[22]

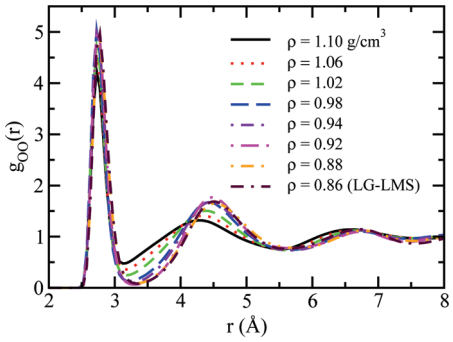

Figure 3. O−O RDFs of bulk water at T = 190 K for densities from ρ = 1.10 g/cm^3 to ρ = 0.86 g/cm^3 (LG-LMS).

4. STRUCTURAL RESULTS

As discussed in the previous section, the study of the phase diagram of bulk water and of the aqueous solution shows the presence of a LLCP in the supercooled region. We now discuss the structural properties of the systems. In the following subsection, we analyze water−water structure both in the bulk and in the solution. Then we study the hydration (ion−water) structure.

A. Water−Water Structure. In Figure 3 we report the O−O radial distribution functions (RDFs) of bulk water at the LLCP temperature for decreasing densities from ρ = 1.10 g/cm^3 to the LG-LMS density ρ = 0.86 g/cm^3. According to our phase diagram, the LLCP in bulk water is located at ρ = 1.06 g/cm^3. As a general trend, there is an increase of the first peak with decreasing density. The second peak from ρ = 0.86 g/cm^3 to ρ = 0.98 g/cm^3 does not substantially change position. As the LLCP is approached, from ρ = 1.02 g/cm^3 it starts to shift to lower distances.

The LLCP is located at ρ = 0.99 g/cm^3 in NaCl(aq); thus, in order to study the structural differences between the LDL and the HDL both in bulk water and in NaCl(aq), we take into account, in the following discussion, the RDFs at two density values which are well above and well below the estimated critical densities, namely ρ = 1.10 g/cm^3 for HDL and ρ = 0.92 g/cm^3 for LDL.

In Figure 4 we compare the water−water RDFs $g_{OO}(r)$, $g_{OH}(r)$, and $g_{HH}(r)$ of bulk water obtained at the thermodynamic conditions in which water is either in the LDL or in the HDL region. The RDFs are plotted for T = 190 K at densities ρ = 0.92 g/cm^3 and ρ = 1.10 g/cm^3, representative of LDL and HDL,

dx.doi.org/10.1021/jp1101237 |J. Phys. Chem. B 2011, 115, 1461–1468

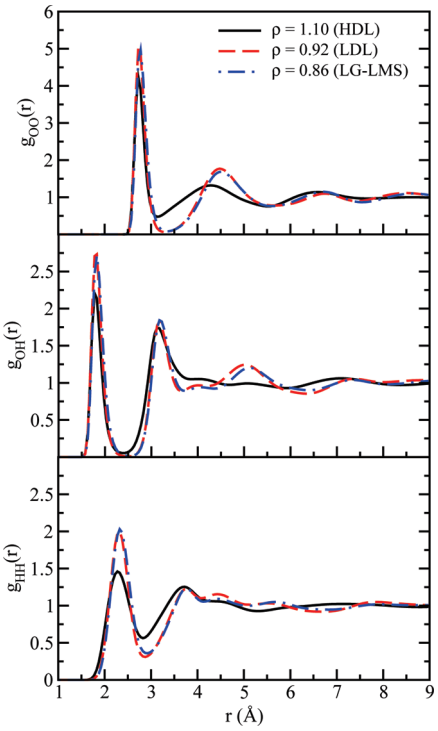

Figure 4. O−O (top panel), O−H (central panel), and H−H (bottom panel) RDFs for bulk water at T = 190 K. Solid lines: ρ = 1.10 g/cm^3 (HDL); dashed lines: ρ = 0.92 g/cm^3 (LDL); dot-dashed lines: ρ = 0.86 g/cm^3 (LG-LMS).

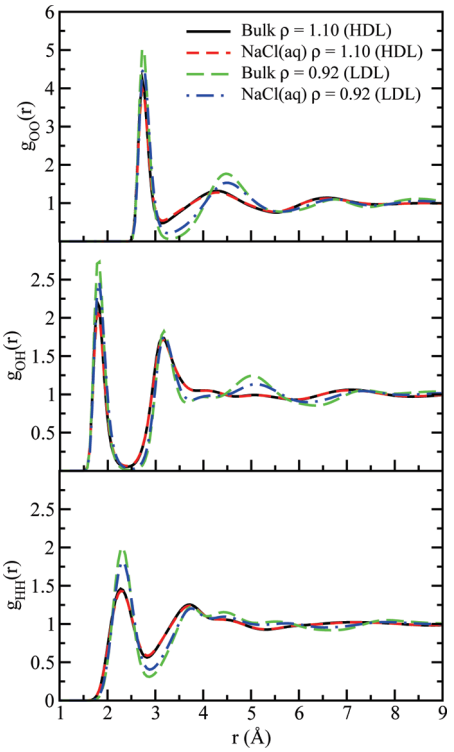

Figure 5. O−O (top panel), O−H (central panel), and H−H (bottom panel) RDFs for bulk water at T = 190 K and for NaCl(aq) at T = 200 K. Solid lines: bulk ρ = 1.10 g/cm^3 (HDL); dashed lines: NaCl(aq) ρ = 1.10 g/cm^3 (HDL); long dashed lines: bulk ρ = 0.92 g/cm^3 (LDL); dot-dashed lines: NaCl(aq) ρ = 0.92 g/cm^3 (LDL).

respectively. The RDFs at density ρ = 0.86 g/cm^3 that represent, at this temperature, the LG-LMS of bulk water are also reported for comparison. We observe for the O−O RDF that the height of the first peak decreases going from LDL to HDL while its position does not change. The second peak instead is markedly different. In HDL its position shifts to lower distances, its height decreases, and its shape broadens, with respect to the LDL. For the $g_{OH}(r)$, the height of the first peak decreases in HDL and it moves to slightly lower distances. This slight shift is conserved between the first and the second shell, while the position and the height of the second shell are fairly similar for HDL and LDL, apart from the appearance of a shoulder between the second and the third shell in HDL. Also note that while the LDL shows a very well-defined third shell, it disappears in HDL. For the $g_{HH}(r)$ also, the first peak of HDL is less intense than that of LDL and slightly shifted to lower distances. Also note a widening of the second shell in the HDL. The overall trend of water−water RDFs and in particular the difference in the second shell of the O−O RDF clearly shows the disruption of hydrogen bonds between the first and second shell of water molecules that occurs in HDL, causing it to have a collapsed second shell with respect to the tetrahedrally coordinated LDL.[28]

The results for HDL and LDL RDFs in bulk water are in good agreement with those found in experiments.[28] It has been shown that the TIP4P model is a very reliable model for the study of the thermodynamics of solid[32] and supercooled liquid water.[22] Our results confirm the validity of the TIP4P model also for the study of the structural properties in the supercooled region.

In Figure 5 we compare the HDL and LDL water−water RDFs for bulk water and for NaCl(aq). In NaCl(aq) the overall shape and positions of the peaks remain similar to those of bulk water in both cases, but some differences are noted for the LDL. The height of the first peak of $g_{OO}(r)$, $g_{OH}(r)$, and $g_{HH}(r)$ is slightly lower for the NaCl(aq) LDL with respect to the correspondent phase in bulk water. Furthermore in $g_{OO}(r)$, the first minimum moves to lower distances in the solution and the height of the second peak is reduced. In $g_{OH}(r)$, the first and the second shell remain similar but the height of the third shell is damped in the NaCl(aq). These results indicate that at this concentration the effect of ions on water−water structure is not strong and all the features found in bulk water are preserved. Nonetheless, LDL seems to be more affected by the presence of ions than HDL. This can be due to a certain degree of disruption of hydrogen bonds induced by the ions. In fact, as shown in Figure 5, the effect of ions is that of reducing the LDL character of water−water structure and making it more similar to that of HDL. These results are in agreement with that observed in our study of the thermodynamics of these systems.[22] In fact, the range of existence of the LDL phase is reduced when ions are added to bulk water.

To complete the comparison between HDL and LDL in bulk water and in NaCl(aq), we report in Figure 6 the quantity

$$h(r) = 4\pi\rho r[0.092g_{OO}(r) + 0.422g_{OH}(r) + 0.486g_{HH}(r) - 1] \quad (3)$$

This correlation function has been obtained in neutron diffraction experiments on the amorphous HDA and LDA phases of water.[45,46] The qualitative agreement shows the existing relation between the LDA/HDA phases of ice with the corresponding LDL/HDL phases of water as already pointed out in simulations

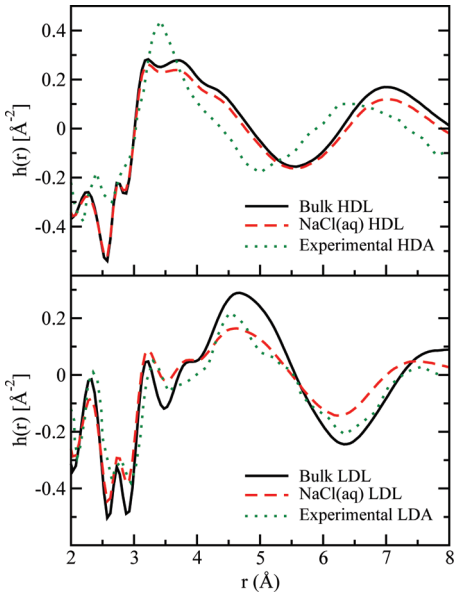

Figure 6. Function $h(r)$; see text for definition. Top panel: bulk HDL (solid line), NaCl(aq) HDL (dashed line), and experimental HDA (dotted line). Bottom panel: bulk LDL (solid line), NaCl(aq) LDL (dashed line), and experimental LDA (dotted line).

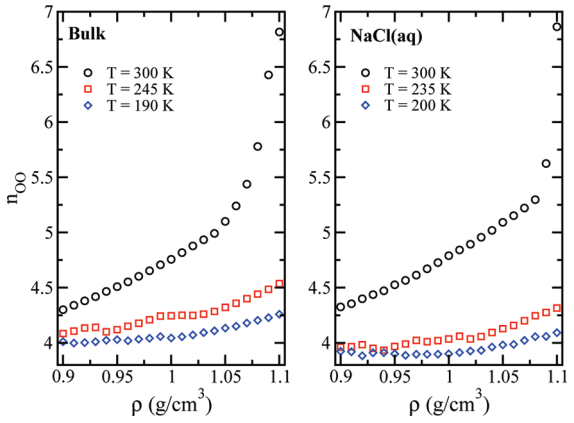

Figure 7. O−O first shell coordination number as a function of density, at constant temperature, for bulk water (left panel) and NaCl(aq) (right panel). The temperatures reported are T = 300 K, T = 245 K, and T = 190 K for bulk water and T = 300 K, T = 235 K, and T = 200 K for NaCl(aq).

of bulk water with the ST2 potential.[15] We observe again that LDL is more influenced by the presence of ions. The modifications to $h(r)$ in fact appear larger in LDL with a significant reduction of the peak at about 4.6 Å and different behavior for long distances, r > 6.5 Å. This confirms the behavior that we observed for LDL, looking at the partial water−water RDFs.

To conclude the analysis of water−water structure, we report in Figure 7 the oxygen−oxygen first shell coordination numbers as a function of density at constant temperature. We report them at the same temperatures that we show in Figure 2 for the potential energy T = 300 K, T = 245 K, and T = 190 K for bulk water and T = 300 K, T = 235 K and T = 200 K for NaCl(aq). The first shell coordination numbers are calculated by integrating the radial distribution function until the first minimum is reached, and thus they represent the average number of first neighbors

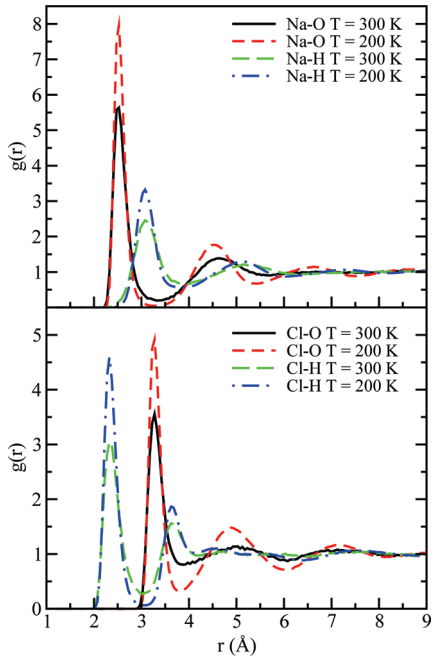

Figure 8. Na−water (top panel) and Cl−water (bottom panel) RDFs at ρ = 1.00 g/cm^3 and at temperatures T = 300 K and T = 200 K.

around an oxygen atom. At high temperatures, the coordination numbers decrease monotonically with the density, without reaching the value of 4, typical of LDL[15] in the spanned range of simulated state points. As temperature is decreased, the isotherms of the coordination numbers approach an asymptotic value of 4 when density decreases. For the lowest temperature, the coordination number reaches the value 4, already at quite high densities in bulk water, and it actually drops slightly below 4 in NaCl(aq). In the case of the first shell coordination numbers, HDL and LDL seem to be affected in a similar way by the presence of ions, with a slight decrease of the average number of first neighbors. Nonetheless, the weakening of the ordered tetrahedral configuration of LDL in the first shell induced by the ions may allow for a reorganization of the bonds that leads to a more packed, HDL-like structure, as we have seen with the RDFs.

B. Hydration Structure. The hydration structure in NaCl(aq) at ambient temperature and in the moderately supercooled region has been the subject of several experimental[29,47,48] and computer simulation works.[49−59] Nonetheless, the hydration behavior close to the LLCP has never been studied previously.

In order to study the general features of the hydration shells, we show in Figure 8 the Na−water and Cl−water RDFs for ρ = 1.00 g/cm^3 at ambient temperature T = 300 K and in the deep supercooled region, at T = 200 K, corresponding to the LLCP temperature in the solution. For all four couples we can observe that there are two well-defined hydration shells. The height of both the first and second peak tends to increase greatly upon supercooling. In the case of Na−O and Cl−O we also observe for the second peak a shift of its position to slightly lower distances at the lowest temperature. These results seem to indicate that upon supercooling the hydration shells tend to stabilize and to become more compact. In the case of the chloride ion, the Cl−O first and second peaks are very well separated from the respective Cl−H peaks, by roughly 1 Å. In the case of the sodium ion the distance is reduced to roughly 0.6 Å and there

dx.doi.org/10.1021/jp1101237 |J. Phys. Chem. B 2011, 115, 1461–1468

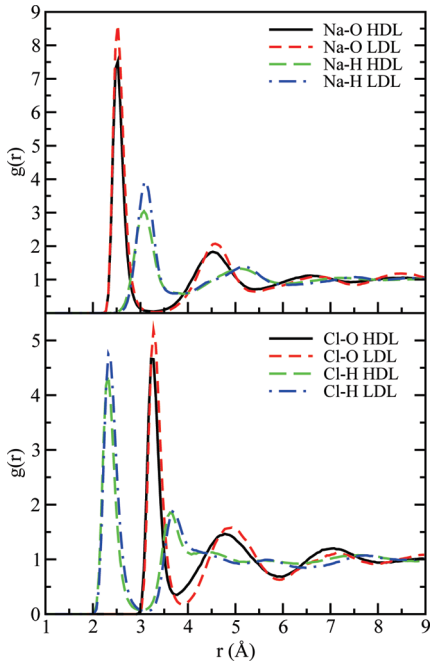

Figure 9. Na−water (top panel) and Cl−water (bottom panel) RDFs for $\rho = 1.10$ g/cm^3 (HDL) and $\rho = 0.92$ g/cm^3 (LDL) at $T = 200$ K.

Table 2. First Shell, n_1, and Second Shell, n_2, Hydration Numbers for Sodium and Chloride Ions in HDL and LDL at the LLCP Temperature, $T_C = 200$ K

atom pair	n_1 HDL	n_1 LDL	n_2 HDL	n_2 LDL
Na−O	5.975	5.957	18.490	15.898
Na−H	15.912	15.364	49.474	43.521
Cl−O	7.214	7.032	23.193	19.378
Cl−H	6.983	7.002	33.177	27.069

is actually an overlap of the Na−O and Na−H hydration shells. For the chloride ion, the hydration structure of the shells is similar to the case of the O−O and O−H structure (see Figure 4 and Figure 5). Thus, we argue that chloride can substitute oxygen in the hydration shells, forming linear hydrogen bonds with oxygen atoms as indicated by the sharp, first Cl−H peak. The Na^+ ion cannot simply substitute the oxygen atom. Its positive charge induces a major rearrangement of the hydration shells that results in more packed structure. The behavior of the hydration shells of Na^+ and Cl^- ions is in good agreement with that found experimentally for ambient temperature in recent neutron diffraction experiments.[29,47]

In Figure 9 we report the Na−water and Cl−water RDFs for the HDL, at $\rho = 1.10$ g/cm^3 and the LDL at $\rho = 0.92$ g/cm^3 and at $T = 200$ K. The hydration shells of sodium ions are not much affected by the HDL or LDL environment of the solvent. An increase of the first and second peak of the Na−O RDF and of the first peak of the Na−H RDF is observed in LDL with respect to HDL but the position of the peaks remains unaltered apart from a very slight shift to higher distances of the second shell of Na−O for the LDL. In the case of the chloride ion, the Cl−H RDF remains unchanged in HDL or LDL but the Cl−O RDF shows some differences. In the LDL the first peak is higher than in HDL and the second peak is both higher and shifted to longer distances. We report in Table 2 the first shell and second shell

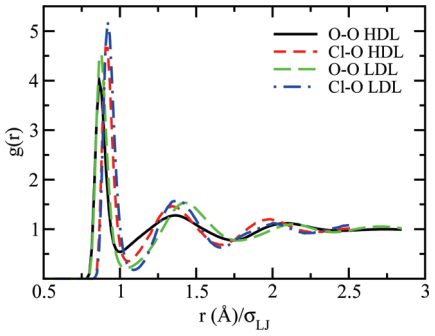

Figure 10. Comparison of HDL and LDL O−O and Cl−O RDFs with distances rescaled by the Lennard−Jones parameter σ.

hydration numbers for the sodium and chloride ions at the LLCP temperature. These numbers have been calculated by numerical integration of the first and second peak of the RDFs plotted in Figure 9. The integration range spans from zero to the first minimum for the first hydration shell and from the first to the second minimum for the second hydration shell. The modifications of the first shell in going from HDL to LDL are practically imperceptible. The second shell appears already sensitive to the HDL and LDL environment as we can deduce from the decrease of hydration numbers in going from HDL to LDL.

As shown in Figure 5 and Figure 6, the ions seem to affect the LDL more than the HDL. The most significant difference in the hydration shells of the ions is noticed in the second shell of the Cl−O RDF. We have also already mentioned that the hydration structure around the chloride ion resembles the O−O and O−H structures (Figure 8) with the chloride ion able to substitute oxygen in shells of other oxygen atoms. To further investigate this possibility and to assess the effect of the chloride ion hydration on HDL/LDL, we plot together in Figure 10 the O−O and Cl−O RDFs for HDL and LDL with distances rescaled by the respective LJ interaction distance parameter σ. For the O−O pair, $\sigma = 3.154$ Å as given in the TIP4P model,[31] and for the Cl−O pair, $\sigma = 3.561$ Å, as reported in Table 1.

In both LDL and HDL the first and the second shell of oxygen atoms are closer in the case of the Cl−O RDF (see also Figure 5 and Figure 9). To make a quantitative comparison, we can examine the distance between the first peak and the second peak of the RDFs, ΔR. In HDL, for the O−O pair, $\Delta R = 0.49$, and for Cl−O, $\Delta R = 0.42$. In LDL, for the O−O pair, $\Delta R = 0.55$, and for Cl−O, $\Delta R = 0.44$ (distances in real units are obtained multiplying ΔR by the respective σ). Thus, in LDL the chloride ion has the major effect in pulling inward its second hydration shell of oxygen. As shown in Figure 4 and Figure 5, the main difference in the structure of HDL and LDL is in the position of the second shell of the O−O RDFs, therefore a possible explanation for why the presence of ions affects the LDL more than the HDL. In fact, the chloride ion can take the place of the central oxygen atom in oxygen shells and can be accommodated in water−water structure at the price of bending hydrogen bonds and pulling the second shell of oxygen closer to the first shell. This can be tolerated in HDL where the molecular structure is already collapsed in the second shell[28], but the LDL structure instead is disrupted. In essence, the substitution of oxygen atoms by chloride atoms together with the hydrogen bond disruption caused by Na^+ forces the LDL structure to become more HDL-like. Hence, we can understand also from a structural point of view why the region of existence of the LDL phase shrinks in the NaCl(aq) with respect to bulk water.

5. CONCLUSIONS

By the use of MD computer simulations, we have studied the structural properties of TIP4P bulk water and of a sodium chloride solution in TIP4P water with concentration c = 0.67 mol/kg. In particular, we were interested in the structural differences between the two phases of water, HDL and LDL, that appear in the deep supercooled region. From our previous work[22] we knew accurately the phase diagrams of these systems and in particular the position of the LLCP.

Our results showed that the TIP4P model can reproduce well the structural properties of the two phases of supercooled liquid water in addition to being a very good potential for the study of liquid[22] and solid[32] water thermodynamics. Comparing water−water RDFs in bulk water and in NaCl(aq), we have seen that the LDL is affected by the presence of ions more than the HDL, as indicated also by the shrinkage of the LDL phase observed in the study of the thermodynamics.

The study of the hydration structure of ions in HDL and LDL revealed that a disturbance to the LDL structure is induced by the substitution of oxygen by chloride ions in coordination shells of other oxygen atoms. The chloride ions in fact pull inward its second shell of oxygen atoms, disrupting the LDL structure. This, together with the hydrogen bond breaking caused by the sodium ion, causes the LDL phase to be less stable in NaCl(aq) solutions and its region of existence in the thermodynamic plane to reduce, with a consequent shift of the liquid−liquid coexistence line and of the LLCP to lower pressures with respect to bulk water.

Since from our thermodynamic results we hypothesize that the LLCP region is above the nucleation line in this solution, an observation of the structural features presented in this paper in X-ray and neutron scattering experiments can also represent a viable route for experimentalists to solve the quest of the LLCP in bulk water. Along this line, experimental indications of a HDL and LDL phase coexistence and LLCP have been recently found.[60]

APPENDIX

The TIP4P model for water is a nonpolarizable potential where three sites are arranged according to the molecular geometry. The two sites representing the hydrogens are positively charged with q_H = 0.52 e; each one forms a rigid bond with the site of the oxygen at a distance of 0.9752 Å. The angle between the bonds is 104.52°. The site of the oxygen is neutral while a fourth site carries the negative charge of the oxygen $q_O = -2q_H$. This site is located in the same plane of the molecule at a distance of 0.15 Å from the oxygen with an angle 52.26° from the OH bond. The intermolecular interactions are represented by eq 1. The LJ parameters are given by σ_{OO} = 3.154 Å and ϵ_{OO} = 0.64852 kJ/mol.

AUTHOR INFORMATION

Corresponding Author
*E-mail: gallop@fis.uniroma3.it.

ACKNOWLEDGMENT

We gratefully acknowledge the computational resources offered by CINECA for the "Progetto Calcolo 891", by the INFN RM3-GRID at Roma Tre University and by the Democritos National Simulation Center at SISSA (Trieste, Italy).

REFERENCES

(1) Poole, P. H.; Sciortino, F.; Essmann, U.; Stanley, H. E. *Nature* **1992**, *360*, 324.
(2) Debenedetti, P. G. *J. Phys.: Condens. Matter* **2003**, *15*, R1669 and references therein..
(3) Debenedetti, P. G.; Stanley, H. E. *Phys. Today* **2003**, *56*, 40.
(4) Sastry, S.; Debenedetti, P. G.; Sciortino, F.; Stanley, H. E. *Phys. Rev. E* **1996**, *53*, 6144.
(5) Angell, C. A. *Science* **2008**, *319*, 582.
(6) Poole, P. H.; Sciortino, F.; Essmann, U.; Stanley, H. E. *Phys. Rev. E* **1993**, *48*, 3799.
(7) Poole, P. H.; Saika-Voivod, I.; Sciortino, F. *J. Phys.: Condens. Matter* **2005**, *17*, L431.
(8) Harrington, S.; Poole, P. H.; Sciortino, F.; Stanley, H. E. *J. Chem. Phys.* **1997**, *107*, 7443.
(9) Yamada, M.; Mossa, S.; Stanley, H. E.; Sciortino, F. *Phys. Rev. Lett.* **2002**, *88*, 195701.
(10) Paschek, D. *Phys. Rev. Lett.* **2005**, *94*, 217802.
(11) Paschek, D.; Rüppert, A.; Geiger, A. *Chem. Phys. Chem.* **2008**, *9*, 2737.
(12) Jedlovszky, P.; Vallauri, R. *J. Chem. Phys.* **2005**, *122*, 081101.
(13) Tanaka, H. *J. Chem. Phys.* **1996**, *105*, 5099.
(14) Liu, Y.; Panagiotopoulos, A. Z.; Debenedetti, P. G. *J. Chem. Phys.* **2009**, *131*, 104508.
(15) Sciortino, F.; Poole, P. H.; Essmann, U.; Stanley, H. E. *Phys. Rev. E* **1997**, *55*, 727.
(16) Mishima, O.; Stanley, H. E. *Nature* **1998**, *392*, 164; **1998**, *396*, 329.
(17) Banarjee, D.; Bhat, S. N.; Bhat, S. V.; Leporini, D. *Proc. Natl. Acad. Sci. U.S.A.* **2009**, *106*, 11448.
(18) Mallamace, F.; Corsaro, C.; Broccio, M.; Branca, C.; Gonzalez-Segredo, N.; Spooren, J.; Chen, S.-H.; Stanley, H. E. *Proc. Natl. Acad. Sci. U.S.A.* **2008**, *105*, 12725.
(19) Mishima, O. *J. Chem. Phys.* **2010**, *133*, 144503.
(20) Miyata, K.; Kanno, H.; Niino, T.; Tomizawa, K. *Chem. Phys. Lett.* **2002**, *354*, 51.
(21) Chatterjee, S.; Debenedetti, P. G. *J. Chem. Phys.* **2006**, *124*, 154503.
(22) Corradini, D.; Rovere, M.; Gallo, P. *J. Chem. Phys.* **2010**, *132*, 134508.
(23) Corradini, D.; Buldyrev, S. V.; Gallo, P.; Stanley, H. E. *Phys. Rev. E* **2010**, *81*, 061504.
(24) Archer, D. G.; Carter, R. W. *J. Phys. Chem. B* **2000**, *104*, 8563.
(25) Carter, R. W.; Archer, D. G. *Phys. Chem. Chem. Phys.* **2000**, *2*, 5138.
(26) Mishima, O. *J. Chem. Phys.* **2005**, *123*, 154506.
(27) Mishima, O. *J. Chem. Phys.* **2007**, *126*, 244507.
(28) Soper, A. K.; Ricci, M. A. *Phys. Rev. Lett.* **2000**, *84*, 2881.
(29) Mancinelli, R.; Botti, A.; Bruni, F.; Ricci, M. A.; Soper, A. K. *J. Phys. Chem. B* **2007**, *111*, 13570.
(30) Neilson, G. W.; Mason, P. E.; Ramos, S.; Sullivan, D. *Phil. Trans. R. Soc. Lond. A* **2001**, *359*, 1575.
(31) Jorgensen, W. L.; Chandrasekhar, J.; Madura, J. D.; Impey, R. W.; Klein, M. L. *J. Chem. Phys.* **1983**, *79*, 926.
(32) Sanz, E.; Vega, C.; Abascal, J. L. F.; MacDowell, L. G. *Phys. Rev. Lett.* **2004**, *92*, 255701.
(33) Jensen, K. P.; Jorgensen, W. L. *J. Chem. Theory Comput.* **2006**, *2*, 1499.
(34) Berendsen, H. J. C.; Postma, J. P. M.; van Gunsteren, W. F.; DiNola, A.; Haak, J. R. *J. Chem. Phys.* **1984**, *81*, 3684.
(35) Smith, W.; Forester, T. R.; Todorov, I. T. *The DL_POLY_2.0 User Manual*; Daresbury Laboratory: Daresbury, UK, 2006.
(36) Franzese, G.; Stanley, H. E. *J. Phys.: Condens. Matter* **2007**, *19*, 205126.
(37) Xu, L.; Kumar, P.; Buldyrev, S. V.; Chen, S.-H.; Poole, P. H.; Sciortino, F.; Stanley, H. E. *Proc. Natl. Acad. Sci. U.S.A.* **2005**, *102*, 16558.
(38) Abascal, J. L. F.; Vega, C. *J. Chem. Phys.* **2010**, *133*, 234502.

(39) Abascal, J. L. F.; Vega, C. *J. Chem. Phys.* **2005**, *123*, 234505.
(40) Souda, R. *J. Chem. Phys.* **2006**, *125*, 181103.
(41) Vega, C.; Sanz, E.; Abascal, J. L. F. *J. Chem. Phys.* **2005**, *122*, 114507.
(42) Kanno, H.; Speedy, R. J.; Angell, C. A. *Science* **1975**, *189*, 880.
(43) Kumar, P.; Buldyrev, S. V.; Starr, F. W.; Giovambattista, N; Stanley, H. E. *Phys. Rev. E* **2005**, *72*, 051503.
(44) Corradini, D.; Gallo, P.; Rovere, M. *J. Chem. Phys.* **2009**, *130*, 154511.
(45) Bellissent-Funel, M. C.; Bosio, L.; Hallbrucker, A.; Mayer, E.; Sridi-Dorbez, R. *J. Chem. Phys.* **1992**, *97*, 1282.
(46) Bellissent-Funel, M. C.; Texeira, J.; Bosio, L.; Dore, J. C. *J. Phys.: Condens. Matter* **1989**, *1*, 7123.
(47) Mancinelli, R.; Botti, A.; Bruni, F.; Ricci, M. A.; Soper, A. K. *Phys. Chem. Chem. Phys.* **2007**, *9*, 2959.
(48) Ohtaki, H. *Monatsh. Chem.* **2001**, *132*, 1237.
(49) Corradini, D.; Gallo, P.; Rovere, M. *J. Chem. Phys.* **2008**, *128*, 244508.
(50) Koneshan, S.; Rasaiah, J. C. *J. Chem. Phys.* **2000**, *113*, 8125.
(51) Chowdhuri, S.; Chandra, A. *J. Chem. Phys.* **2001**, *115*, 3732; **2003**, *118*, 9719.
(52) Patra, M.; Karttunen, M. *J. Comput. Chem.* **2004**, *25*, 678.
(53) Lenart, P. J.; Jusufi, A.; Panagiotopoulos, A. Z. *J. Chem. Phys.* **2007**, *126*, 044509.
(54) Alejandre, J.; Hansen, J.-P. *Phys. Rev. E* **2007**, *76*, 061505.
(55) Lynden-Bell, R. M.; Rasaiah, J. C.; Noworyta, J. P. *Pure Appl. Chem.* **2001**, *73*, 1721.
(56) Zhu, S.-B.; Robinson, G. W. *J. Chem. Phys.* **1992**, *97*, 4336.
(57) Kim, J. S.; Yethiraj, A. *J. Phys. Chem. B* **2008**, *112*, 1729.
(58) Du, H.; Rasaiah, J. C.; Miller, J. D. *J. Phys. Chem. B* **2007**, *111*, 209.
(59) Joung, I. S.; Cheatham, T. E., III. *J. Phys. Chem. B* **2008**, *112*, 9020.
(60) Huang, C.; Weiss, T. M.; Nordlund, D.; Wikfeldt, K. T.; Pettersson, L. G. M.; Nilsson, A. *J. Chem. Phys.* **2010**, *133*, 134504.